Proc. Natl. Acad. Sci. USA
Vol. 91, pp. 12701–12705, December 1994
Biophysics

Coherent nuclear dynamics at room temperature in bacterial reaction centers

(photosynthesis/electron transfer/femtosecond spectroscopy/stimulated emission)

MARTEN H. VOS[†], MICHAEL R. JONES[‡], C. NEIL HUNTER[‡], JACQUES BRETON[§], AND JEAN-LOUIS MARTIN[†]

[†]Laboratoire d'Optique Appliquée, Institut National de la Santé et de la Recherche Médicale Unité 275, Centre National de la Recherche Scientifique Unité de Recherche Associée 1406, Ecole Polytechnique-Ecole Nationale Supérieure de Techniques Avancées, 91120 Palaiseau, France; [‡]Department of Molecular Biology and Biotechnology, Krebs Institute for Biomolecular Research and Robert Hill Institute for Photosynthesis, University of Sheffield, Western Bank, Sheffield S10 2UH, United Kingdom; and [§]Département de Biologie Cellulaire et Moléculaire, Section de Bioénergétique, Commissariat à l'Energie Atomique Saclay, 91191 Gif-sur-Yvette Cedex, France

Communicated by George Feher, September 8, 1994

ABSTRACT **A room-temperature study is reported of the femtosecond spectral evolution of the stimulated emission band of the primary electron-transfer precursor P* in bacterial photosynthesis. The study was performed with membranes of the antenna-deficient RCO1 mutant of *Rhodobacter sphaeroides*. A time-dependent red shift, reflecting nuclear motion out of the Franck–Condon region of the excited state, is resolved. Analysis of oscillatory features persisting for >1 ps in the kinetics revealed main frequencies of the activated motions at 30, 84, 145, and 192 cm^{-1}. The oscillations occur on the time scale of primary electron transfer. Our results set a lower limit for the vibrational dephasing time in P* that is not compatible with the usual assumption in theoretical treatments of complete vibrational relaxation prior to electron transfer, even at room temperature.**

The primary charge separation in photosynthetic reaction centers (see refs. 1 and 2 for reviews) takes place between a donor (a bacteriochlorophyll dimer, P) and an acceptor (a bacteriopheophytin, H_L) at a center-to-center distance of ≈17 Å. The time scale of this reaction, about 3 ps at room temperature (3, 4), is extremely fast for a direct reaction spanning such a distance. As an additional monomeric bacteriochlorophyll (B_L) is located in a configuration more or less bridging P and H_L (5, 6), it has been put forward by many workers that the presence of B_L may be the key to the extreme speed and efficiency of the reaction. In particular, it has been proposed that the state $P^+B_L^-$ is a real intermediate that is shorter lived than the P* precursor excited state (7, 8) or, alternatively, that it is a virtual intermediate that mediates the reaction in a superexchange mechanism (9–11). Combinations of both mechanisms have also been proposed (12, 13). Very detailed analyses of short-lived transient absorption kinetics in terms of rate constants are at the center of the ongoing debate on the experimental basis for these models.

From a theoretical point of view, these models are based on the conventional description of nonadiabatic electron transfer (ET), in which nuclear and electronic factors can be separated and contribute as independent factors to the ET rate (14–16). A crucial assumption in this description is that the vibrational modes of the precursor state of ET are thermally populated on the time scale of the reaction, which implies that vibrational relaxation and, if relaxation occurs via inelastic interactions with the bath, vibrational dephasing take place prior to ET.

In this paper we will address the question of whether the hypothesis of vibrational dephasing prior to electron transfer is justified at room temperature and whether parameters other than a linear combination of exponentials may interfere in the analysis of ultrafast optical kinetics. Previous reports concerned the observation, at low temperature, of oscillatory features in bacterial reaction centers reflecting coherent motions in the P* state (17, 18). These specific low-frequency motions persist on the time scale of the primary ET reaction [≈1 ps at cryogenic temperatures (19)]. Observation of these motions has invalidated the assumption that, at least in wild-type reaction centers, the excited state is vibrationally relaxed during the reaction at cryogenic temperatures. However, the majority of the studies concerning the primary charge separation have been performed at room temperature—i.e., closer to the conditions under which the reaction center operates *in vivo* than the low-temperature studies where the coherent motions were detected. Therefore an assessment of the character of the vibrational motions during the ET reaction at room temperature is warranted.

In an earlier study, no oscillations reflecting coherent vibrational motion were detected at room temperature in functional reaction centers (17). This study was performed with a relatively long pump pulse (80 fs) and only at a single wavelength in the stimulated emission band. In a later study of mutant reaction centers which do not perform charge separation, it was shown that the relative amplitude of the oscillatory modulation of the kinetics was strongly wavelength dependent within the stimulated emission band (18). In this mutant, oscillatory features were observed up to 290 K, albeit with a strongly reduced amplitude compared with those seen at cryogenic temperatures (17). Stimulated by these results, we have reinvestigated the oscillatory kinetics in the entire stimulated emission band of wild-type reaction centers. Further important experimental improvements are (*i*) the use of membranes of the antenna-deficient RCO1 mutant of *Rhodobacter sphaeroides* (20), where the oscillations dampen somewhat slower than in isolated reaction centers (21); (*ii*) the use of short (30-fs) pump pulses; and (*iii*) independent calibration of zero time delay. In a very recent paper (22), we have shown that under these improved conditions, at 10 K, in addition to the 15-cm^{-1} features reported earlier (17), pronounced oscillatory features in the region near 120 cm^{-1} can be observed that also bear the wavelength characteristics of excited-state vibrational motions. The initial red shift of the stimulated emission band, out of the region where it completely overlaps with the ground-state absorption band, was also resolved and demonstrated to be associated with coherent motion. In the present paper we show that, even at room temperature, the phase of vibrational motions coupled to the P → P* transition persists for several

The publication costs of this article were defrayed in part by page charge payment. This article must therefore be hereby marked "*advertisement*" in accordance with 18 U.S.C. §1734 solely to indicate this fact.

Abbreviations: ET, electron transfer; FT, Fourier transform.

periods and that different vibrational modes can be visualized by modifying the characteristics of the excitation pulse.

MATERIALS AND METHODS

Intracytoplasmic membranes from the *R. sphaeroides* RCO1 mutant, in which the genes coding for both the LHI and LHII light-harvesting proteins are deleted, were prepared as described (23) and suspended in 20 mM Tris buffer (pH 8.0). The concentration of the sample was adjusted to an OD_{860} of ≈0.35 (optical path length, 1 mm). The quinone electron acceptor Q_A was reduced by the addition of 50 mM dithiothreitol. The sample was continuously moved perpendicular to the pump and probe beams.

Pulse shaping and calibration of zero time delay are described in detail elsewhere (22). Very briefly, the dispersion in the pump and probe beams was compensated and the time resolution was essentially determined by the pump pulse. The pump pulses were centered at 870 nm. They had a 30-fs full width at half maximum (fwhm) and the spectrum shown in Fig. 1. Where mentioned explicitly in the text, spectrally narrow (10 nm), 100-fs-fwhm pump pulses were used.

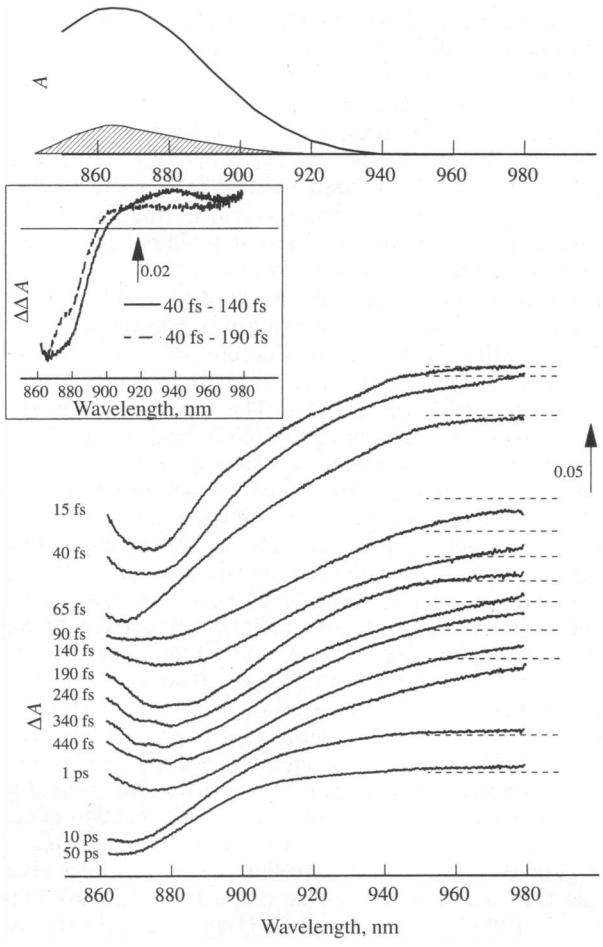

FIG. 1. Ground-state absorption spectrum (*Upper*) and transient absorption spectra at various delay times (*Lower*). The jitter in the timing of the spectra is <10 fs and the systematic error in the delay times is <20 fs. The marked delay times correspond to 920 nm, the optimal compression wavelength of the probe pulses. The remaining chirp after compression of the probe pulse is such that the spectral parts of the probe pulse at 870 and 970 nm correspond to delay times ≈30 fs earlier than that at 920 nm. The hatched area in *Upper* represents the spectrum of the pump pulse. (*Inset*) Double difference spectra, obtained by subtracting the transient spectra at 140 fs and 190 fs from that at 40 fs. A positive signal corresponds to enhanced stimulated emission with respect to t = 40 fs.

RESULTS

Transient Spectra. Transient spectra in the spectral region 860–980 nm were taken at various delay times (Fig. 1). The negative absorption features are due to bleaching of the ground-state P absorption band and stimulated emission from the photoinduced P* state. The general features of the spectra at longer delay times (longer than ≈300 fs) are in agreement with other reported spectra obtained on wild-type reaction centers with a lower time resolution (24, 25), and their most apparent time evolution consists of the overall decay of the stimulated emission band on a picosecond time scale. The high time resolution of this study allows us to monitor, in addition, the initial shaping of the emission band. In a way qualitatively similar to the evolution of the sharper spectral features at 10 K (22), the stimulated emission is seen to shift to the red between ≈40 fs (i.e., after completion of the pump pulse) and ≈140 fs, whereupon the wave packet on the excited state turns and the stimulated emission band shifts back to the blue. The double difference spectra of the *Inset* of Fig. 1 highlight this shift after t = 40 fs (note the displaced zero crossing point in the two spectra).

Kinetics. The dynamic character of the evolution of the stimulated emission band is further illustrated by the subpicosecond kinetics shown in Fig. 2. The rise of the red side of the stimulated emission band is clearly delayed compared with the appearance of the stimulated emission/bleaching at the blue side. In contrast to the kinetics at low temperature (22), the apparent rise kinetics at the red side are also markedly slower (less steep) than those at the blue side (see also Fig. 5 *Inset*). The kinetics further display small but clear oscillatory features (main period ≈ 250 fs). The phases of these features are opposite on both sides of the stimulated emission band and they disappear between 918 and 898 nm (compare with Fig. 5). Such behavior is characteristic for

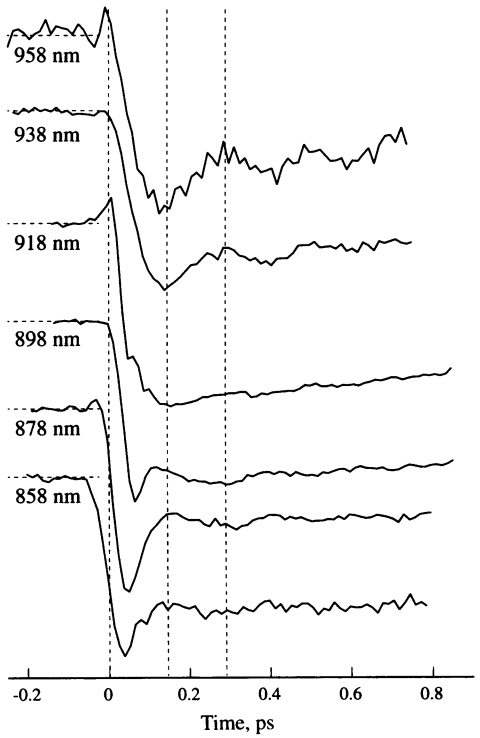

FIG. 2. Subpicosecond kinetics at selected wavelengths. The amplitudes are normalized. The jitter in the timing of the kinetics is <10 fs and the systematic error in the delay times is <20 fs. The dashed lines are introduced to facilitate the comparison of the phase of the oscillations at different wavelengths.

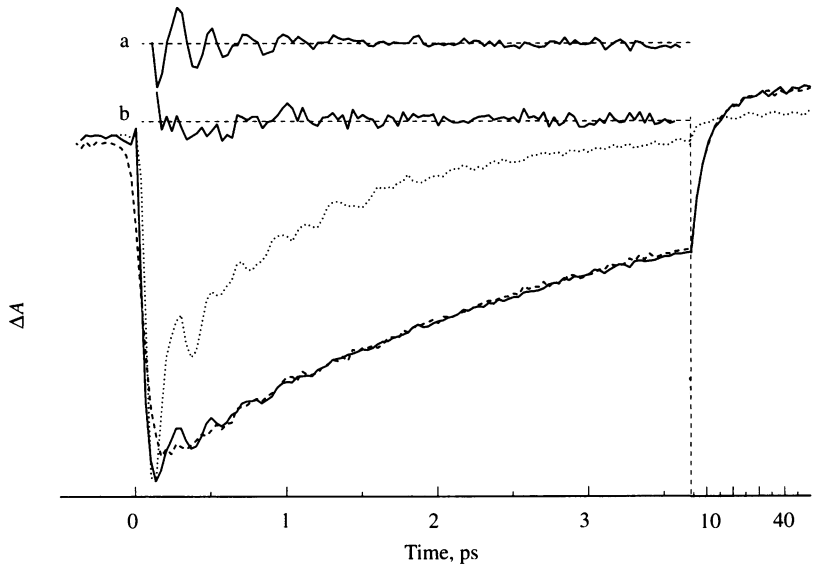

FIG. 3. Dual time-base kinetics (4 ps and 46 ps) at 938 nm at room temperature (solid and dashed curve) and 10 K (dotted curve). The dashed curve was taken with a 100-fs pump pulse with a spectral width of 10 nm centered at 870 nm. Upper traces: oscillatory parts (expanded 2×) of the room temperature kinetics (traces a and b, 30-fs and 100-fs pump pulse, respectively), obtained by fitting the data with a biexponential decay function (time constants, 2.8 and 10 ps; amplitude ratio, 2:1).

coherent vibrational motion on the excited-state potential energy surface (18, 22).

Fig. 3 shows the kinetics at 938 nm on an extended time scale. At least four maxima in the oscillatory pattern can be observed before they are damped at 1–1.5 ps. The oscillatory pattern is similar to that of the kinetics at 10 K (22), which are also shown for comparison (Fig. 3, dotted line). However, at room temperature the initial amplitude of the oscillations is considerably smaller and the features are visible for a more limited time span, despite the slower overall decay of P*.

When P is excited with a longer (100-fs) and spectrally narrower (10-nm) pump pulse, the ≈250-fs-period oscillations cannot be observed. Instead, a small but significant lower-frequency (see below) feature becomes apparent. For both traces, a biexponential function was needed to accurately fit the decay in the kinetic portion where the oscillations are damped. In this way the oscillatory parts were isolated (Fig. 3, top traces) and their Fourier transforms (FTs) are shown in Fig. 4. In the FT spectrum associated with the 30-fs pump-pulse experiment, the main vibrational band peaks at 145 cm^{-1} and additional peaks are resolved at 84 and 192 cm^{-1}. This spectrum is qualitatively similar to that observed at 10 K (Fig. 4*A*, dotted line), but the peaks are less well resolved, the higher frequency components are relatively enhanced, and no significant frequency feature is observed below 50 cm^{-1}. By contrast, in the vibrational spectrum of the oscillatory part of the 100-fs pump-pulse experiment (Fig. 4*B*), the FT bands observed with 30-fs pulses are absent, and the only significant feature is a band at ≈30 cm^{-1}.

The overall kinetics of decay of P* stimulated emission are also wavelength dependent. This is shown in Fig. 5, where the kinetics at 878, 908, and 938 nm (obtained with 30-fs pump pulses) are normalized on the portion of the decay curves at $t > 3.5$ ps. The overall kinetics are slower on the blue side of the spectrum (the fastest component in the kinetic fit shifts from ≈2.8 ps to ≈3.8 ps between 938 nm and 878 nm), corresponding to a gradual blue shift of the transient spectrum. A similar effect has been observed at 10 K (data not shown). This effect could be due to heterogeneity in the overall ET kinetics or to a relaxation of the transient P* state (13, 26).

DISCUSSION

Previously, coherent nuclear motion at room temperature has been observed in bacteriorhodopsin (27) and in heme proteins (28). In those studies, the observed motions took place on the ground-state potential energy surface, coherently populated via the impulsive stimulated Raman effect, and they could not be involved in a physiological reaction. The results presented in this paper constitute evidence for intramolecular coherent nuclear motion at a physiological temperature in an excited state that is the direct precursor of a biological reaction. In particular, our results show that it is possible that concerted motions play an important role in primary ET in the photosynthetic reaction center, which serves as a model system for biological ET.

Vibrational Motion. The onset of the shift of the emission band and subsequent oscillatory spectral dynamics are qualitatively similar to those observed at 10 K (22). However, the apparent rise kinetics at the red side of the emission band are

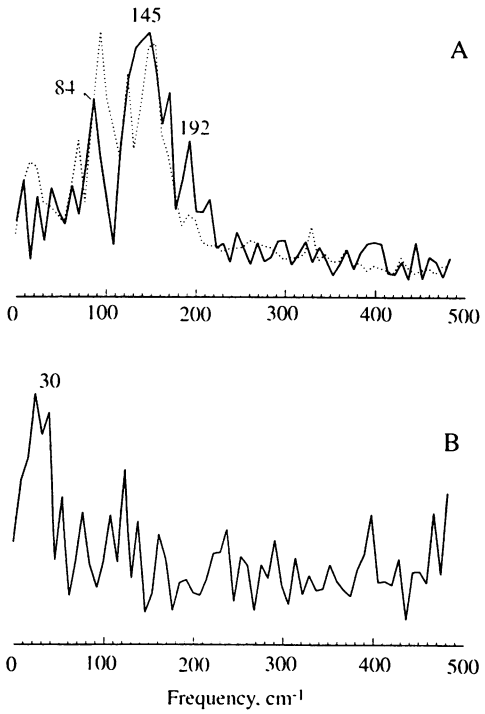

FIG. 4. FTs of the oscillatory parts of the kinetics at 938 nm of Fig. 3 obtained with pump pulses of 30 fs (*A*, solid curve) and 100 fs (*B*). For comparison, the same analysis for the data at 10 K (30-fs pump pulses) is shown (*A*, curve). The amplitudes of the spectra are normalized to the peak amplitude of the corresponding kinetics; the spectrum at 10 K was then divided by 3.

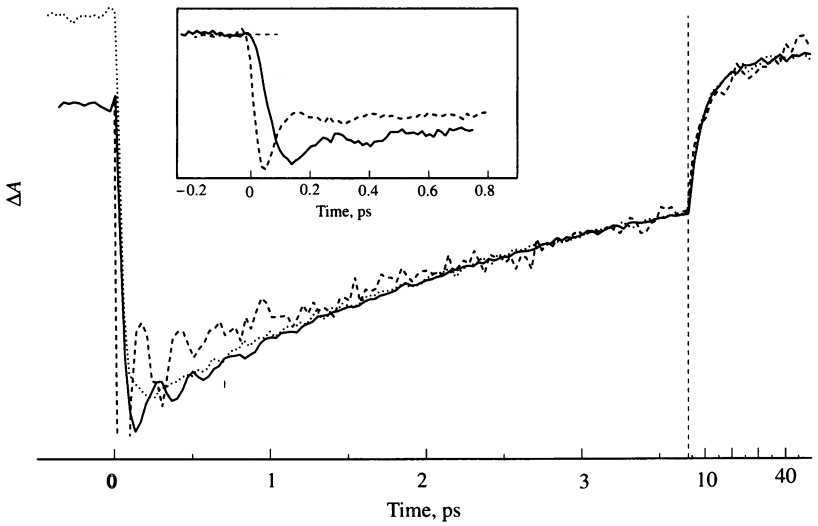

FIG. 5. Dual time-base kinetics (4 ps and 46 ps) at 878 nm (dashed curve), 908 nm (dotted curve), and 938 nm (solid curve). The data are normalized on the second time-base ($t > 3.6$ ps) part. For clarity the kinetics at 878 nm are truncated. (*Inset*) Superimposed and amplitude-normalized early-time kinetics at 878 nm (dashed curve) and 938 nm (solid curve) from Fig. 3.

slower and the amplitude of the oscillations is markedly lower at room temperature. This is probably due to the ground-state thermal population of higher vibrational levels at room temperature ($kT = \approx 240\ cm^{-1}$). This population is projected into a somewhat broader initial wave packet in the excited state by the pump pulse (width $\approx 400\ cm^{-1}$) and especially will give rise to a less well-defined initial phase of the wave packet. The low amplitude prevents the observation of overtone oscillatory features near the center of the band (≈908 nm), which are expected to be yet an order of magnitude lower in amplitude (18, 22).

Interestingly, the lowest-frequency oscillations (≈30 cm^{-1}) give rise to significant FT components only when a spectrally narrower and longer pump pulse is used (Figs. 3 and 4; see also ref. 17). The effect seems more pronounced at room temperature than at 100 K (22). Although the stronger interference of the low-frequency modes with the overall decay of P* at 100 K (22) makes it difficult to quantify the temperature dependence of this effect, it may be an indication of the involvement of anharmonicity. It is possible that the low-frequency mode is a ground-state mode populated by impulsive stimulated Raman excitation, for which pump-pulse length effects are expected (29), although the phase of the low-frequency feature is consistent with excited-state dynamics.

The peak frequencies in the FT spectra are similar to those observed at low temperature and compare well (22) with results from room-temperature resonance Raman (30) and low-temperature photochemical hole-burning (31–33) spectroscopy. However, it should be noted that the present technique is unique in its ability to resolve the vibrational structure of the excited state underlying the P → P* transition at room temperature. Two notable differences between the observations at 10 K and at room temperature are (*i*) the apparent upshift of the lowest-frequency band to ≈30 cm^{-1} at room temperature (observed with 100-fs pulses), which is near the lowest resolvable peak in the resonance Raman spectrum of P at 36 cm^{-1} (30), and (*ii*) the congestion of two peaks, which at 10 K were observed at 122 and 153 cm^{-1}, to a single broad band at room temperature peaking at ≈145 cm^{-1} (observed with 30-fs pulses), presumably a manifestation of frequency broadening of those bands by inhomogeneity and anharmonicity.

Vibrational Relaxation and ET. The time over which the oscillations are discernible, 1–1.5 ps (Fig. 3), sets a *minimal* value for the vibrational dephasing time by quasielastic or inelastic energy exchange with the bath. The oscillatory phase correlations in individual reaction centers may be preserved for a longer time if the observed damping is due to dispersion of the frequencies (by anharmonicity and/or site inhomogeneity) of the activated modes. The differences in damping between 10 K and room temperature may thus be due to differences in frequency dispersion and collisional dephasing. An indication that collisional dephasing is not the main source of damping comes from a study on the influence of the environment of the reaction center on the damping of the oscillations—i.e. detergent-solubilized reaction centers compared with membrane-bound reaction centers (21). This influence was found to be not very dependent on the temperature, whereas collisional dephasing by coupling to the solvent is expected to be more effective at higher temperatures.

Vibrational dephasing occurs prior to (in the case of pure dephasing interactions) or simultaneous with (in the case of vibrational relaxation interactions) thermal equilibration. A recent NMR study indicated that the protein environment of P is extremely rigid and displays elastic behavior (34), which may indicate that chromophore–protein interactions have a dominantly pure dephasing character. Taking these facts together, we conclude that thermalization takes place on the time scale of at least 1 ps but probably occurs more slowly than this, even at room temperature. As a consequence, the population of the P* vibrational manifold from which the primary ET reaction occurs in wild-type reaction centers is not determined (only) by the temperature, but rather by the initial population of the vibrational levels. Most of the derivations of ET theory assume that no dynamic processes are occurring on the time scale of the reaction. This hypothesis is clearly not supported in the case of primary ET in reaction centers.

The possibility of ET from a vibrationally unrelaxed P* state has been discussed in theoretical terms in several papers (33, 35–38). In particular, Skourtis *et al.* (37) argued that a mechanism whereby vibrational relaxation takes place on the same time scale as ET will be very efficient and robust against changes in the free-energy gap of the reaction and in temperature. On the other hand Bixon and Jortner (39) argued that activationless or inverted-region ET may be only weakly dependent on the medium relaxation dynamics, although coherence effects were not treated in their paper.

The low-frequency modes that are coupled to the P → P* transition probably have a rather delocalized character (21, 22). The significant differences between the FT spectra of wild-type *R. sphaeroides* and those of the D_{LL} mutant of *Rhodobacter capsulatus* (18), which bears several mutations distant from P and which lacks H_L, are consistent with such a character. The chromophores not constituting P, including B_L, are likewise also involved to a certain extent in these

motions, and this will be reflected in the early-time kinetics in regions where these chromophores absorb.

This observation may be particularly pertinent for the debate on the role of a state $P^+B_L^-$ as a real intermediate state in ET between P* and $P^+H_L^-$. As the time scales of decay of P* and appearance of $P^+H_L^-$ are not very different (3, 4), an intermediate state can be rationalized in a rate scheme only if it is short lived compared to the lifetime of P* (7, 8, 11–13). The use of rate constants to describe the primary charge separation kinetics is based on transitions between thermodynamically equilibrated states. We have shown here that even at room temperature the P* state is not thermally relaxed and that the short-lived character (<1 ps) of a putative $P^+B_L^-$ state makes it unlikely that this state would be thermally relaxed either. In particular, if the nuclear movement along the reaction coordinate(s) is coherent, the probability of ET will be time dependent and a rate description is inappropriate. Even in the case that the coherent motions are orthogonal to the reaction coordinates, they may be reflected in the optical transients and interfere in the analysis of the kinetics in terms of rate constants. The use of long pump and probe pulses experimentally smears out the oscillatory features but cannot *a priori* prevent the possibility that damped low-frequency motions contribute to the kinetics.

Conclusion. We have demonstrated vibrational coherence in the excited state of bacterial reaction centers at room temperature. The vibrational motions persist at least in part during the primary ET reaction. Whereas the present findings have characterized the vibrational motions activated by the capture of photons, it remains to be determined whether these motions are directly involved in the ET reaction, and the ensemble of available experimental data, including those from hole-burning, resonance Raman, femtosecond, and other spectroscopic studies, have yet to be merged in a unique comprehensive picture of the primary ET reaction. Several apparent inconsistencies among those various studies, such as that regarding the total displacement of the excited-state potential energy surface (40), remain to be resolved.

M.H.V. was supported by Commissariat à l'Energie Atomique, Centre National de la Recherche Scientifique, and Fondation pour la Recherche Médicale during the course of this work. M.R.J. and C.N.H. acknowledge support from the Wellcome Trust and the European Community. M.R.J. is an Agriculture and Food Research Council Senior Research Fellow.

1. Martin, J.-L. & Vos, M. H. (1992) *Annu. Rev. Biophys. Biomol. Struct.* **21,** 199–222.
2. Woodbury, N. W. & Allen, J. M. (1994) in *Anoxygenic Photosynthetic Bacteria*, eds. Blankenship, R. E., Madigan, M. T. & Bauer, C. E. (Kluwer, Dordrecht), in press.
3. Martin, J.-L., Breton, J., Hoff, A. J., Migus, A. & Antonetti, A. (1986) *Proc. Natl. Acad. Sci. USA* **83,** 957–961.
4. Woodbury, N. W., Becker, M., Middendorf, D. & Parson, W. W. (1985) *Biochemistry* **24,** 7516–7521.
5. Deisenhofer, J. P., Epp, O., Miki, K., Huber, R. & Michel, H. (1984) *J. Mol. Biol.* **180,** 385–398.
6. Allen, J. P. & Feher, G. (1984) *Proc. Natl. Acad. Sci. USA* **81,** 4795–4799.
7. Holzapfel, W., Finkele, U., Kaiser, W., Oesterhelt, D., Scheer, H., Stilz, H. U. & Zinth, W. (1990) *Proc. Natl. Acad. Sci. USA* **87,** 5168–5172.
8. Arlt, T., Schmidt, S., Kaiser, W., Lauterwasser, C., Meyer, M., Scheer, H. & Zinth, W. (1993) *Proc. Natl. Acad. Sci. USA* **90,** 11757–11761.
9. Michel-Beyerle, M. E., Plato, M., Deisenhofer, J., Michel, H., Bixon, M. & Jortner, J. (1988) *Biochim. Biophys. Acta* **932,** 52–70.
10. Warshel, A., Creighton, S. & Parson, W. W. (1988) *J. Phys. Chem.* **92,** 2697–2701.
11. Kirmaier, C. & Holten, D. (1991) *Biochemistry* **30,** 609–613.
12. Chan, C.-K., DiMagno, T. J., Chen, L. X.-Q., Norris, J. R. & Fleming, G. R. (1991) *Proc. Natl. Acad. Sci. USA* **88,** 11202–11206.
13. Nagarajan, V., Parson, W. W., Davis, D. & Schenck, C. (1993) *Biochemistry* **32,** 12324–12336.
14. Marcus, R. A. & Sutin, N. (1985) *Biochim. Biophys. Acta* **811,** 265–322.
15. Bixon, M. & Jortner, J. (1989) *Chem. Phys. Lett.* **159,** 17–20.
16. Moser, C. C., Keske, J. M., Warncke, K., Farid, R. S. & Dutton, P. L. (1992) *Nature (London)* **355,** 796–802.
17. Vos, M. H., Lambry, J.-C., Robles, S. J., Youvan, D. G., Breton, J. & Martin, J.-L. (1991) *Proc. Natl. Acad. Sci. USA* **88,** 8885–8889.
18. Vos, M. H., Rappaport, F., Lambry, J.-C., Breton, J. & Martin, J.-L. (1993) *Nature (London)* **363,** 320–325.
19. Fleming, G. R., Martin, J.-L. & Breton, J. (1988) *Nature (London)* **333,** 190–192.
20. Jones, M. R., Visschers, R. W., van Grondelle, R. & Hunter, C. N. (1992) *Biochemistry* **31,** 4458–4465.
21. Vos, M. H., Jones, M. R., McGlynn, P., Hunter, C. N., Breton, J. & Martin, J.-L. (1994) *Biochim. Biophys. Acta* **1186,** 117–122.
22. Vos, M. H., Jones, M. R., Hunter, C. N., Breton, J., Lambry, J.-C. & Martin, J.-L. (1994) *Biochemistry* **33,** 6750–6757.
23. Jones, M. R., Heer-Dawson, M., Mattioli, T. A., Hunter, C. N. & Robert, B. (1994) *FEBS Lett.* **339,** 18–24.
24. Taguchi, A. K. W., Stocker, J. W., Alden, R. G., Causgrove, T. P., Peloquin, Boxer, S. G. & Woodbury, N. W. (1992) *Biochemistry* **31,** 10345–10355.
25. Kirmaier, C., Holten, D., Bylina, E. & Youvan, D. C. (1988) *Proc. Natl. Acad. Sci. USA* **85,** 7562–7566.
26. Nagarajan, V., Parson, W. W., Gaul, D. & Schenck, C. (1990) *Proc. Natl. Acad. Sci. USA* **87,** 7888–7892.
27. Dexheimer, S. L., Wang, Q., Peteanu, L. A., Pollard, W. T., Mathies, R. A. & Shank, C. V. (1992) *Chem. Phys. Lett.* **188,** 61–66.
28. Zhu, L., Li, M., Huang, M., Sage, J. T. & Champion, P. M. (1994) *Phys. Rev. Lett.* **72,** 301–304.
29. Pollard, W. T., Dexheimer, S. L., Wang, Q., Peteanu, L. A., Shank, C. V. & Mathies, R. A. (1992) *J. Phys. Chem.* **96,** 6147–6158.
30. Shreve, A. P., Cherepy, N. J., Franzen, S., Boxer, S. G. & Mathies, R. A. (1991) *Proc. Natl. Acad. Sci. USA* **88,** 11207–11211.
31. Johnson, S. G., Tang, D., Jankowiak, R., Hayes, J. M., Small, G. J. & Tiede, D. M. (1990) *J. Phys. Chem.* **94,** 5849–5855.
32. Lyle, P. A., Kolaczkowski, S. V. & Small, G. R. (1993) *J. Phys. Chem.* **97,** 6924–6933.
33. Middendorf, T. R., Mazzola, L. T., Gaul, D. F., Schenck, C. C. & Boxer, S. G. (1991) *J. Phys. Chem.* **95,** 10142–10151.
34. Fischer, M. R., de Groot, H. J. M., Raap, J., Winkel, C., Hoff, A. J. & Lugtenburg, J. (1992) *Biochemistry* **31,** 11038–11049.
35. Jortner, J. (1980) *Biochim. Biophys. Acta* **594,** 193–230.
36. Jean, J. M., Friesner, R. A. & Fleming, G. R. (1992) *J. Chem. Phys.* **96,** 5827–5842.
37. Skourtis, S. S., da Silva, A. J. R., Bialek, W. & Onuchic, J. N. (1992) *J. Phys. Chem.* **96,** 8034–8041.
38. Gehlen, J. N., Marchi, M. & Chandler, D. (1994) *Science* **263,** 499–502.
39. Bixon, M. & Jortner, J. (1993) *Chem. Phys.* **176,** 467–481.
40. Cherepy, N. J., Shreve, A. P., Moore, L. J., Franzen, S., Boxer, S. G. & Mathies, R. A. (1994) *J. Phys. Chem.* **98,** 6023–6029.